

Dynamics of riverine CO₂ in the Yangtze River fluvial network and their implications for carbon evasion

Lishan Ran¹, Xi Xi Lu^{2,3,*}, Shaoda Liu²

5 ¹Department of geography, the University of Hong Kong, Pokfulam Road, Hong Kong

²Department of geography, National University of Singapore, 117570, Singapore

³College of Environment & Resources, Inner Mongolia University, Hohhot, 010021, China

*Correspondence: geoluxx@nus.edu.sg

10 **Abstract:** Understanding riverine carbon dynamics is critical for not only better estimates of various carbon fluxes but also evaluating their significance in the global carbon budget. As an important pathway of global land-ocean carbon exchange, the Yangtze River has received less attention regarding its vertical carbon evasion compared with lateral transport. Using long-term water chemistry data, we calculated CO₂ partial pressure ($p\text{CO}_2$) from pH and alkalinity and
15 examined its spatial and temporal dynamics and the impacts of environmental settings. With alkalinity ranging from 415 to >3400 $\mu\text{eq L}^{-1}$, the river waters were supersaturated with dissolved CO₂, generally 2–20 folds the atmospheric equilibrium (i.e., 390 μatm). Changes of $p\text{CO}_2$ were collectively controlled by carbon inputs from terrestrial ecosystems, hydrological regime, and rock weathering. High $p\text{CO}_2$ values were observed spatially in catchments with
20 abundant carbonate presence and seasonally in the wet season when recent-fixed organic matter was exported into the river network. In-stream processing of organic matter facilitated CO₂ production and sustained the high $p\text{CO}_2$, although the alkalinity presented an apparent dilution effect with water discharge. The decreasing $p\text{CO}_2$ from the smallest headwater streams through tributaries to the mainstem channel illustrates the significance of direct terrestrial carbon inputs
25 in controlling riverine CO₂. With a basin-wide mean $p\text{CO}_2$ of $2662 \pm 1240 \mu\text{atm}$, substantial CO₂

evasion from the Yangtze River fluvial network is expected. Future research efforts are needed to quantify the amount of CO₂ evasion and assess its biogeochemical implications for watershed-scale carbon cycle. In view of the Yangtze River's relative importance in global carbon export, its CO₂ evasion would be significant for global carbon budget.

30 **Keywords:** CO₂ partial pressure ($p\text{CO}_2$); riverine carbon cycle; spatial and temporal patterns; CO₂ evasion; Yangtze River

1. Introduction

Inland waters, including rivers, streams, lakes, wetland, and reservoirs, have recently been
35 recognized as active components of the global carbon (C) cycle, transporting, storing, and processing huge amounts of terrestrially-derived carbon (Aufdenkampe et al., 2011; Cole et al., 2007; Raymond et al., 2013; Richey et al., 2002; Weyhenmeyer et al., 2015; Borges et al., 2015). With a higher CO₂ partial pressure ($p\text{CO}_2$) than the atmospheric equilibrium (i.e., 390 μatm), inland waters are mostly net carbon sources to the atmosphere. Published studies show that the
40 annually degassed CO₂ from inland waters is estimated to almost entirely compensate the total annual carbon uptake by ocean systems (Wanninkhof et al., 2013; Regnier et al., 2013). Global estimates of CO₂ evasion from rivers and streams range from 0.56 to 1.8 PgC yr⁻¹ (Aufdenkampe et al., 2011; Raymond et al., 2013; Lauerwald et al., 2015). It is apparent that these results vary considerably and are associated with great uncertainties. The most recent estimate of 0.65 PgC
45 yr⁻¹ by Lauerwald et al. (2015) accounts for only 36% of the efflux estimated by Raymond et al. (2013). While both studies have used the same hydrochemical database (GloRiCh), it should be

noted that Raymond et al. (2013) used all the calculated $p\text{CO}_2$ values whereas Lauerwald et al. (2015) used only 18% of the sampling locations. Among the numerous factors contributing to current CO_2 evasion uncertainties, a principal reason is the absence of a spatially explicit $p\text{CO}_2$ data set that covers the full spectrum of the global river and stream network.

Existing global maps of CO_2 evasion from fluvial network are typically generated on the basis of incomplete spatial coverage of $p\text{CO}_2$, in which Asian rivers are heavily underrepresented (e.g., Aufdenkampe et al., 2011; Battin et al., 2009; Lauerwald et al., 2015; Raymond et al., 2013). Due to lack of direct *in situ* measurements, simplified extrapolation is normally used to predict $p\text{CO}_2$ in and CO_2 evasion from Asian river systems. Consequently, the estimation accuracy is problematic and even erroneous. For example, for the Yellow River in East Asia, while the calculated $p\text{CO}_2$ from river water chemistry is $2800 \mu\text{atm}$ (Ran et al., 2015a), the modeled $p\text{CO}_2$ by Lauerwald et al. (2015) is 30% lower (i.e., $<2000 \mu\text{atm}$). A much lower estimate of $<700 \mu\text{atm}$ can be derived from the $p\text{CO}_2$ map produced in Raymond et al. (2013). Such great discrepancies are largely because riverine $p\text{CO}_2$ is highly site-specific and affected by a wide range of environmental factors (e.g., Abril et al. 2015; Teodoru et a., 2015). Asian rivers are significant contributors to global carbon flux as a result of high soil erosion and particulate organic carbon export, accounting for 40% of the global carbon flux from land to sea (Schlünz and Schneider, 2000; Hope et al., 1994). Estimating the amount of CO_2 degassed from Asian rivers is critical for global CO_2 evasion assessments. Recent work in Mekong and Yellow rivers has demonstrated high $p\text{CO}_2$ and CO_2 effluxes (Alin et al., 2011; Ran et al., 2015b), further

highlighting the necessity of incorporating the currently underrepresented Asian rivers into global carbon budget assessments.

70

As an important carbon contributor to the West Pacific Ocean, the Yangtze River has received widespread attention in fluvial carbon export at various spatial and temporal scales. Studies of flux estimates of different carbon species date back to the early 1980s (Cauwet and Mackenzie, 1993; Gan et al., 1983; Milliman et al., 1984; Wang et al., 2012; Zhang et al., 2014; Ittekkot, 1988).

75

Intensive observations covering seasonal variability show that the Yangtze River transports approximately 20 Mt of C per year into the oceans (Wu et al., 2007; Bao et al., 2015). Contrary to the long history of lateral export measurements, however, few studies have examined the vertical carbon exchange between the river system and the atmosphere (Li et al., 2012; Zhao et al., 2013; Chen et al., 2008). This is by nature largely due to the differences in sampling strategy.

80

Unlike the lateral export that only involves measurements on the mainstem or at specific sites near the river mouth, quantifying basin-wide CO₂ evasion requires a spatially explicit *p*CO₂ data set encompassing the entire fluvial network. Any attempts of using limited local measurements to up-scale to the watershed scale are challenging and subject to large uncertainties. This has impacted the understanding of the riverine carbon cycle within the Yangtze River watershed as

85

well as its links to the atmosphere and ocean systems.

By using long-term water chemistry data measured in the Yangtze River watershed, we calculated the riverine *p*CO₂ from pH and alkalinity. In combination with hydrologic and

lithologic information, the objectives of this study were to 1) investigate the spatial and temporal
90 patterns of $p\text{CO}_2$ under ‘natural’ processes before significant human perturbations, mainly dam
impoundment and land-use change since the 1990s; 2) to explore the couplings between $p\text{CO}_2$
and environmental settings by investigating environmental and geomorphologic controls. Based
on the obtained $p\text{CO}_2$, we further evaluated its biogeochemical implications for CO_2 evasion. In
view of the Yangtze River’s role in global fluvial export of water, sediment, and carbon (Syvitski
95 et al., 2005; Wang et al., 2012), its contribution to the global CO_2 evasion from river systems is
likely significant. This $p\text{CO}_2$ database is thus helpful to examine the spatial distribution of global
riverine $p\text{CO}_2$ and to refine estimates of global CO_2 evasion.

2. Material and methods

100 2.1 The Yangtze River basin

With a length of 6380 km, the Yangtze River is the longest river in China and the third longest in
the world. The river originates on the Tibetan Plateau and flows eastward through the Sichuan
Basin and the Middle-Lower Reach Plains, before emptying into the East China Sea (Fig. 1a). Its
drainage area is 1.81 million km^2 . The Yangtze River basin is mainly overlain by sedimentary
105 rocks that are composed of marine carbonates, evaporites, and continental deposits. Carbonate
sedimentary rocks are widely distributed within the watershed and are particularly abundant in
the Wujiang, Yuanjiang, and Hanjiang tributary catchments (Fig. 1b). Siliciclastic sedimentary
rocks are also widely present in the basin while metamorphic rocks are mainly scattered in the
middle-lower reach (Fig. 1b). The Yangtze River is joined by a number of large tributaries,

110 including the Yalongjiang, Daduhe, Minjiang, Jialingjiang, Wujiang, Yuanjiang, Xiangjiang,
Hanjiang, and Ganjiang rivers (Fig. 1a).

Figure 1

Except the headwater region characterized by high elevation and cold climate (annual mean
temperature $<4^{\circ}\text{C}$), the remaining watershed is affected by subtropical monsoons with the annual
115 mean temperature in the middle-lower reach varying from 16 to 18 $^{\circ}\text{C}$ (Chen et al., 2002).
Rainfall is the major source of water discharge, whereas snowfall supply is only significant in the
ice-covered upstream mountainous areas. With a mean precipitation of 1100 mm yr^{-1} , the
precipitation is spatially highly variable, decreasing from 1644 mm yr^{-1} in the lower reach, to
1396 mm yr^{-1} in the middle reach, and 435 mm yr^{-1} in the upper reach (Chetelat et al., 2008).
120 Approximately 60% of the annual precipitation falls during the wet season from June to
September. Affected by summer monsoons, the wet season generally occurs earlier in the middle
and lower reaches than in the inland upper reach. Water discharge from the upper to the lower
reach presents a strong seasonal variability (Fig. 2). Monthly peak discharge occurs in July and
can be 5–7 times greater than the lowest discharge in the dry season (October to May). The mean
125 discharge at Datong station is 28,200 $\text{m}^3 \text{s}^{-1}$ (see its location in Fig. 3b), and consequently the
Yangtze River annually discharges 889 km^3 of water into the ocean (Yang et al., 2002).

Figure 2

2.2 Water chemistry data

Concentrations of alkalinity, major ions, and dissolved silica measured at 359 stations in the
130 Yangtze River watershed (Fig. 1a) during the period 1960s–1985 were retrieved from the

Hydrological Yearbooks, which were yearly produced by the Yangtze River Conservancy Commission (YRCC) for internal use. Concomitant environmental variables measured at each sampling event, including pH, water temperature, and discharge, were also extracted from the yearbooks. The water samples for pH and temperature measurement were taken in the same
135 period as these for ion analysis. The sampling frequency ranged from 1 to 14 times per month depending on flow conditions. While sampling at some stations during 1966–1975 was less frequent, ~80% of the 359 stations have been continuously sampled for at least 10 years, starting from the early 1970s. To avoid severe river pollution by human activity, only the samples collected prior to 1985 were used. In addition, samples with a pH lower than 6.5 were manually
140 discarded (498 measurements; predominantly in the lower reach) because the calculated $p\text{CO}_2$ would be greatly biased due to contributions of noncarbonated alkalinity such as organic acid anions (Abril et al., 2015; Hunt et al., 2011). Because reservoir trapping and increased water residence time can remarkably alter the physical and biogeochemical properties of running water (Kemenes et al., 2011; Barros et al., 2011), the stations located inside or shortly below reservoirs
145 were also intentionally removed. Given the tidal influences, mainstem stations downstream of Datong, 626 km inland from the coast, were also excluded, as were the stations in the delta region that were affected either by tides or by intersections with other rivers via artificial canals. Based on these selection criteria, 339 stations, including 13 mainstem stations and 326 tributary stations, were retained and 47,809 water chemistry measurements in total were compiled. The
150 discarded samples owing to $\text{pH} < 6.5$ accounted for approximately 1% of the considered measurements. No sampling station was excluded solely because it had $\text{pH} < 6.5$ samples only.

Chemical analyses of water samples were performed under the authority of YRCC following the standard procedures and protocols described by Alekin et al. (1973) and the American Public Health Association (1985). While pH and temperature were measured in the field, the alkalinity was determined by acid titration. Detailed sampling and analysis procedures were presented in Chen et al. (2002). One important issue regarding historical records is data reliability. No assessment reports on quality assurance and quality control are available in the hydrological yearbooks. An effective evaluation approach is to compare the hydro-chemical differences for samples collected at the same station but by different agencies. The Wuhan station on the Yangtze mainstem has also been monitored under the United Nations GEMS/Water Programme since 1980 (only yearly means available at <http://www.unep.org/gemswater>). The pH value from the yearbooks agreed well with that measured by the GEMS/Water Programme with <1.8% differences, while the alkalinity discrepancy between the two data sets is larger (Table 1). The yearbooks report a slightly higher alkalinity than the GEMS/Water Programme results by 7.6–13.9%, indicating that the yearbook reports are reliable for $p\text{CO}_2$ calculation. High data quality of the yearbook reports can also be validated from comparison of major dissolved elements measured by the two agencies at Wuhan station (see Chen et al., 2002).

Table 1

2.3 Calculation of $p\text{CO}_2$

The conventional method of calculating $p\text{CO}_2$ from pH and alkalinity was used. With ~90% of the pH values ranging from 7.1 to 8.3 suggestive of natural process for the Yangtze River,

bicarbonates were assumed equivalent to alkalinity (Amiotte-Suchet et al., 2003), accounting for 96% of the total alkalinity. As a result of low dissolved organic carbon (i.e., <250 μM ; Liu et al., 2016), impact of organic acids on alkalinity is predicted to be small. The $p\text{CO}_2$ was then calculated using CO2SYS program (Lewis and Wallace, 1998). However, using this method would produce biased extreme values that are unrealistic in natural river systems (Hunt et al., 2011; Weyhenmeyer et al., 2015). We thus reported median values per sampling station instead of means to avoid the impact of erroneous extreme results. The results were summarized in the Supplement (Table S1).

3. Results

3.1 Spatio-temporal variability of alkalinity and $p\text{CO}_2$

Except the excluded measurements, pH in the Yangtze River waters varied from 6.5 to 9.2 with 96% of the pH measurements ranging from 7.3 to 8.3 (Table 2). Higher pH values (i.e., >7.8) were spatially measured in the headwater streams and the Hanjiang catchments (see Fig. 1a for location). In comparison, the tributaries in the southern part of the watershed exhibited relatively low pH values. For the mainstem channel (Table 2), the median pH showed a significant downstream decrease from 8.29 to 7.55 ($r^2 = 0.77$; $p < 0.001$). The alkalinity varied from 415 to >3400 $\mu\text{eq L}^{-1}$ (Fig. 3a). Higher alkalinity (i.e., >2500 $\mu\text{eq L}^{-1}$) was observed in the upper reach and the upper part of the middle reach (Fig. 3a), in particular the carbonate-rich tributary catchments (e.g., the Jialingjiang, Wujiang, and Hanjiang rivers). In contrast, the lower part of

the middle reach (mainly the Ganjiang River) and the lower reach showed a lower alkalinity of $<2000 \mu\text{eq L}^{-1}$. The average alkalinity over the whole watershed was $2210 \pm 1023 \mu\text{eq L}^{-1}$.

195

Figure 3 and Table 2

The calculated $p\text{CO}_2$ varied by a magnitude of 2 with the highest $p\text{CO}_2$ being $24,432 \mu\text{atm}$. At 95% of the stations, the $p\text{CO}_2$ was higher than $1000 \mu\text{atm}$, generally 2–20 folds the atmospheric $p\text{CO}_2$. Only one station in the upper reach showed a median $p\text{CO}_2$ lower than the atmosphere. In the mainstem, the $p\text{CO}_2$ increased from $\sim 700 \mu\text{atm}$ at the uppermost station to $3800 \mu\text{atm}$ at Nanjing near the river mouth (Table 2). Averaged over all stations, the basin-wide $p\text{CO}_2$ was $2662 \pm 1240 \mu\text{atm}$. To better illustrate its spatial variability, we modeled the $p\text{CO}_2$ for the whole stream network using the Kriging interpolation method in ArcGIS 10.1 (Esri, USA) with the assumption that the station-based $p\text{CO}_2$ was representative of the surrounding streams. Similar to alkalinity, the $p\text{CO}_2$ presented significant spatial variations (Fig. 3b). The Yangtze mainstem near the headwater region and the Yalongjiang catchment showed the lowest $p\text{CO}_2$, generally $<1000 \mu\text{atm}$. In comparison, the carbonate-rich tributaries in the southern part of the watershed had high $p\text{CO}_2$ values. With an areal coverage of 83% by carbonate sedimentary rocks, the Wujiang catchment presented the highest median $p\text{CO}_2$ than other tributaries, averaging $3550 \pm 1356 \mu\text{atm}$. In the lower reach, the $p\text{CO}_2$ was $3988 \pm 1244 \mu\text{atm}$ on average, which is inconsistent with its relatively low alkalinity of $<2000 \mu\text{eq L}^{-1}$ (Fig. 3a). It is worth noting that the $p\text{CO}_2$ in Hanjiang catchment was lower than expected, given its high alkalinity ($>2500 \mu\text{eq L}^{-1}$). Differences in pH in these catchments are likely a principal cause of these inconsistencies.

200

205

210

In addition, the $p\text{CO}_2$ also showed strong temporal variability. Fig. 4 presents an example of
215 $p\text{CO}_2$ changes at Datong station on the mainstem channel. Despite considerable inter-annual
variations that could change by a factor of 5, the annual $p\text{CO}_2$ declined steadily during the >20-
year-long sampling period ($r^2 = 0.18$; $p < 0.05$) (Fig. 4a). This trend is pronounced even if the
anomalously high values in the late 1960s are excluded. Indeed, more than half of the evaluated
stations, mainly in the middle-lower reach, showed a significant decreasing trend at the 95%
220 confidence level. In contrast, gradual increases were observed at some tributary stations in the
upper reaches. Seasonally, the $p\text{CO}_2$ in the wet season was on average 30% higher than that in
the dry season (Fig. 4b), and greater fluctuation ranges could be observed in wet seasons.

Figure 4

3.2 Correlations with hydro-geochemical variables

225 Fig. 5 presents two representative examples showing responses of alkalinity and $p\text{CO}_2$ to
hydrological regimes. Changes of alkalinity at both stations reflected a clear dilution effect. High
alkalinity concentrations were measured in low flow periods when groundwater was the major
contributor to runoff (Figs. 5a and 5c). Checking all stations indicated that the alkalinity at 98%
of the stations decreased exponentially with increasing water discharge after the onset of the wet
230 season. In contrast, the $p\text{CO}_2$ presented diverse relationships with water changes (Figs. 5b and
5d). There was no discernible dependence of $p\text{CO}_2$ on flow in the mainstem, while a positive
correlation was widely observed in small tributaries. Although only two stations were plotted

here, these diverse responses of alkalinity and $p\text{CO}_2$ to flow changes were widespread within the watershed, in particular for $p\text{CO}_2$ between mainstem and small tributaries.

235

Figure 5

In order to elucidate the impacts of rock weathering on $p\text{CO}_2$, we selected three typical tributary catchments with differing rock compositions (Table 3). The Wujiang catchment is mainly underlain by carbonate sedimentary rocks (83%) and the Ganjiang catchment by siliciclastic sedimentary rocks (65%), whereas the Jialingjiang catchment lies in the middle regarding the areal coverage of the two rocks (Table 3 and Fig. 1b). As the most typical weathering products of carbonate and siliciclastic sedimentary rocks, we plotted Ca^{2+} and dissolved silica (expressed as SiO_2) against $p\text{CO}_2$, respectively (Fig. 6). For the three catchments with contrasting rock compositions, the $p\text{CO}_2$ showed different responses to Ca^{2+} and SiO_2 . In Wujiang catchment, the log-transformed $p\text{CO}_2$ (i.e., $\lg(p\text{CO}_2)$) presented a significant negative correlation with Ca^{2+} concentration ($p < 0.001$) (Fig. 6). This negative correlation became less apparent with decreasing carbonate coverage in Jialingjiang and Ganjiang catchments. In contrast, while the $\lg(p\text{CO}_2)$ exhibited a positive correlation with SiO_2 in Jialingjiang and Ganjiang catchments characterized by high coverage of siliciclastic sedimentary rocks, no clear relation between $\lg(p\text{CO}_2)$ and SiO_2 was detected in Wujiang catchment (Fig. 6). However, when plotting $p\text{CO}_2$ against Ca^{2+} and SiO_2 for the entire Yangtze River watershed, there was no discernable relationship between $p\text{CO}_2$ and both variables (Fig. S1 in the Supplement).

240

245

250

Figure 6 and Table 3

4. Discussion

4.1 Uncertainty analysis of $p\text{CO}_2$

255 As an important parameter for CO_2 evasion estimation, an accurate riverine $p\text{CO}_2$ is essential to quantify CO_2 evasion and explore its biogeochemical implications for carbon cycle at different scales. Compared with direct measurement by means of membrane equilibration or headspace technique, the conventional $p\text{CO}_2$ calculation from alkalinity has been criticized for causing biases (Long et al., 2015; Hunt et al., 2011). Huge overestimations (i.e., >100%) have been
260 reported in rivers with organic-rich and acidic waters due to combined effects of high organic acids and low buffering capacity of carbonate systems at low pH (Abril et al., 2015).

Unfortunately, there were no organic carbon information in the yearbooks, and measurements of dissolved organic carbon (DOC) in the Yangtze River started in the early 1980s. Its DOC ranging from 130 to 180 μM was relatively low compared with other major world rivers (Bao et
265 al., 2015; Wang et al., 2012). Our recent sampling also shows that the mean DOC is 160 μM for the mainstem and 200 μM for major tributaries (Liu et al., 2016). Given the neutral to basic pH range and the alkalinity variations, we believe the impact of organic acids is minimal, although a slight overestimation may have occurred as suggested by Abril et al. (2015). Our recent $p\text{CO}_2$ measurements in the mainstem and major tributaries using a membrane contactor (Qubit DCO_2
270 System, Qubit Biology Inc., Canada) also indicate that the calculated $p\text{CO}_2$ results are consistent with the measured values with only ~8% differences (Liu et al., 2016).

Furthermore, this $p\text{CO}_2$ calculation method is sensitive to pH changes. High accuracy of pH measurements is critical to reduce the associated uncertainty. Similar to other water chemistry

275 records (i.e., Butman and Raymond, 2011; Lauerwald et al., 2015; Weyhenmeyer et al., 2015),
the retrieved pH was reported with a precision of one decimal place. If the uncertainties in pH
measurement accuracy are assumed to 0.1 pH units, the calculated $p\text{CO}_2$ would be
underestimated by 26% or overestimated by 21%. To minimize human-induced disturbances in
the chemical equilibrium of natural waters, we excluded the samples with $\text{pH} < 6.5$ and treated
280 them as being significantly polluted. This arbitrary exclusion may have generated biased
estimates of $p\text{CO}_2$ for the whole river network in general and some natural rivers characteristic
of low pH in particular (Wallin et al., 2014). Considering the higher alkalinity than the
GEMS/Water Programme results, the propagated uncertainty ranges from 14% (underestimation)
to 27% (overestimation). As China's major industrial and agricultural regions, impact of human
285 activity within the watershed, including sewage inputs and chemical fertilizer usage to a lesser
extent, may have altered its chemical compositions and pH. In view of the small number of
discarded measurements (1% of the total) and the high buffering capacity of carbonate alkalinity
and low DOC contents, the calculated $p\text{CO}_2$ is reasonable and can be used for further CO_2
evasion estimation.

290

4.2 Environmental impacts on alkalinity and $p\text{CO}_2$

Export of alkalinity in river systems was affected by hydrological regime with a clear dilution
effect (Fig. 5). The average alkalinity was 35% lower in the wet season than in the dry season. In
both the mainstem and the tributaries, the higher alkalinity during low flow periods in dry
295 seasons (Figs. 5a and 5c) illustrated the contribution of groundwater recharge in providing

abundant alkalinity. With widespread carbonate presence, groundwater in the Yangtze River watershed was rich in dissolved inorganic carbon (DIC). Recent studies show that the alkalinity of typical karst groundwater in the watershed is in the range of 3300–4200 $\mu\text{eq L}^{-1}$ (Li et al., 2010b; Li et al., 2010a). With reduced relative contribution of groundwater in the wet season, the high alkalinity was diluted by local rain events that carried lower DIC contents. Spatially, the dilution effect was more pronounced in the upper reach than the middle-lower reach. This may have revealed the response of alkalinity production to land cover. Catchments with a higher forest cover normally exhibit a stronger dilution effect than cropland catchments (Raymond and Cole, 2003). While cropland was the major land-use type in the middle-lower reach accounting for 53.5% of the total catchment area, forest cover in the upper Yangtze River watershed was much higher (37.3%) than the middle-lower reach (30.4%; data are from Data Center for Resources and Environmental Sciences for the 1980s).

Riverine dissolved CO_2 originates primarily from terrestrial ecosystem respiration, groundwater input, and in-stream processing of land-derived organic matter (Wallin et al., 2013; Lynch et al., 2010). Different from alkalinity showing a clear dilution effect, the stable $p\text{CO}_2$ in the Yangtze mainstem likely reflected the impact of different biogeochemical processes (Fig. 5b). Compared to the dry season in which the $p\text{CO}_2$ was mainly controlled by DIC inputs from groundwater, the elevated $p\text{CO}_2$ in the wet season suggested the influence of organic carbon transport and decomposition. Owing to strong erosion and leaching of recent-fixed organic matter, its organic carbon content in the wet season is significantly higher and the age much younger (Wang et al.,

2012;Zhang et al., 2014). Rapid mineralization of the labile fraction of organic carbon can increase the $p\text{CO}_2$. A recent study indicates that, while ~60% of the recent-fixed carbon entering the Yangtze River in wet seasons can be quickly degraded, the degradation ratio is only 31% in
320 dry seasons (Wang et al., 2012). On the other hand, the increasing $p\text{CO}_2$ with flow in tributaries indicated enhanced supply of fresh dissolved CO_2 during high flow periods (Fig. 5d). For tributaries with more homogeneous catchment settings, decomposition of soil organic matter can provide abundant dissolved CO_2 (Liu et al., 2016;Li et al., 2012), generating a positive $p\text{CO}_2$ response to water discharge. Presence of wetlands and floodplains also affects river
325 biogeochemistry (Teodoru et al., 2015). Affected by dam impoundment, the catchment upstream of Yunxian station is characteristic of widespread wetlands and floodplains. Consequently, the enhanced connectivity between river and wetlands/floodplains along aquatic continuum, especially during wet seasons, have maintained its high $p\text{CO}_2$ levels (Abril et al., 2014). For $p\text{CO}_2$ in the mainstem (Fig. 5b), it is likely because the increased dissolved CO_2 inputs by soil
330 organic matter decomposition from one region has been counteracted by low $p\text{CO}_2$ waters derived from other regions. This is highly possible given its heterogeneous catchment settings in terms of vegetation cover, soil type, and rainfall intensity. Furthermore, the large catchment implies a long travel time of land-derived organic carbon during fluvial delivery (3–5 months). Coupled with limited floodplains along the mainstem channel (see discussion below), direct
335 inputs of CO_2 from soil respiration would be relatively low whereas strong CO_2 evasion in lower-order turbulent tributaries might have already exhausted dissolved CO_2 . Therefore, its $p\text{CO}_2$ dynamics appeared to be independent of hydrograph.

The spatial distribution of alkalinity overlapped well with the outcrops of carbonate sedimentary
340 rocks (Figs. 1b and 3a), with ~60% of the high alkalinity concentrations measured in carbonate
catchments. Using Ca^{2+} as a proxy of rock weathering, the strong correlation between Ca^{2+} and
alkalinity suggested the dominant role of weathering in controlling alkalinity and DIC export
(Fig. 7). This is consistent with the significant impact of weathering on alkalinity as observed in
other rivers (Raymond and Cole, 2003; Humborg et al., 2010). Particularly, given the higher
345 susceptibility of carbonates to weathering than silicates (Goudie and Viles, 2012), the abundant
carbonate presence in Wujiang catchment helped to sustain its high alkalinity and $p\text{CO}_2$ (Table
3). However, the negative correlation in Fig. 6a is contradictory to the common belief that
carbonate dissolution will likely cause an elevated $p\text{CO}_2$ (Marcé et al., 2015; Teodoru et al.,
2015). Given the significant correlation between Ca^{2+} and alkalinity, the decreasing $p\text{CO}_2$ with
350 increasing Ca^{2+} is probably due to pH variability that may have offset the impact of weathering-
induced DIC inputs in controlling $p\text{CO}_2$ (Fig. S2). A slight pH increase would result in a reduced
 $p\text{CO}_2$ as this calculation method is sensitive to pH fluctuations (Laruelle et al., 2013).

The positive correlation between $p\text{CO}_2$ and SiO_2 in Jialingjiang and Ganjiang catchments
355 demonstrated the impact of DIC export by silicate weathering. Despite the high silicate
weathering rate in Ganjiang catchment, its alkalinity represented only one third of that in the
other two catchments (Table 3). Apparently, its high $p\text{CO}_2$ of $2642 \pm 626 \mu\text{atm}$ was primarily the
result of its low pH (~6% lower). Overall, the catchments with more carbonate presence

presented higher $p\text{CO}_2$ values (Figs. 1 and 3b). Because weathering products are typical for
360 groundwater, this also suggests that riverine $p\text{CO}_2$ has a strong groundwater signature. Different
from the positive response of $p\text{CO}_2$ to discharge at Yunxian station reflecting the importance of
connectivity between river and wetlands/floodplains (Fig. 5d), the decreasing $p\text{CO}_2$ at Xiajiang
station with discharge is indicative of the impact of groundwater input on riverine carbon
dynamics (Figs. S3a and 6f). Particularly, in dry seasons with groundwater dominating the runoff
365 (Fig. S3b), SiO_2 can explain ~25% of the $p\text{CO}_2$ variability in sub-catchments covered mainly
with siliciclastic sediment rocks, comparable to the results by Humborg et al. (2010) in Sweden.
The indiscernible $p\text{CO}_2\text{-Ca}^{2+}$ and $p\text{CO}_2\text{-SiO}_2$ relationship for the entire watershed may be
attributed to the spatial heterogeneity in lithology that has obscured the signature (Fig. S1).
While both positive and negative relationships existed in sub-catchments with predominant
370 carbonate or siliciclastic sediment rocks (Fig. 6), these relationships may have counteracted each
other when all data points were plotted together.

Figure 7

Because $p\text{CO}_2$ was calculated from alkalinity, its spatial variability reflected largely the export of
the latter. The inconsistencies between $p\text{CO}_2$ and alkalinity in Hanjiang catchment were likely
375 caused by dam operation (Fig. 3). By altering the physical and biogeochemical properties of
flowing water, dam trapping could cause a greatly declined $p\text{CO}_2$ as a result of photosynthetic
 CO_2 fixation and increased pH (Ran et al., 2015a). The Danjiangkou Reservoir (storage: 17.5
 km^3) on the upper Hanjiang River was constructed in 1968. Unfortunately, the retrieved data for
the Hanjiang River started from the 1970s, rendering it impossible to compare the $p\text{CO}_2$

380 differences between pre- and post-dam periods. An indirect evidence is that an elevated pH
within the reservoir has been measured (7.95–8.33; Li et al., 2009) relative to the 1970s
(7.84±0.15). In the lower reach near the estuary (Fig. 3b), more pronounced net-heterotrophy and
human activity could explain its high $p\text{CO}_2$. Settling down of particulate organic matter coupled
with nutrient-rich water plume from offshore can accelerate CO_2 production. Chen et al. (2008)
385 concluded that aerobic respiration of heterotrophic ecosystems was the primary determinant of
the high $p\text{CO}_2$ in the inner Yangtze estuary. Moreover, the lower Yangtze River watershed was
highly populated. Inputs of acids from agricultural fertilizer, sewage, and acid deposition have
also decreased pH and shifted the carbonate system towards CO_2 (Duan et al., 2007; Chen et al.,
2002), generating high $p\text{CO}_2$ values regardless of its relatively low alkalinity.

390

4.3 Geomorphological controls on alkalinity and $p\text{CO}_2$

To illustrate the geomorphological controls, the used 339 stations were aggregated by stream
order based on their spatial positions. Both alkalinity and $p\text{CO}_2$ showed a decreasing trend from
the smallest headwater streams through tributaries to the Yangtze mainstem (Fig. 8). The average
395 decrease of alkalinity and $p\text{CO}_2$ were $94 \mu\text{eq L}^{-1}$ and $266 \mu\text{atm}$, respectively. Higher alkalinity
and $p\text{CO}_2$ in the headwater streams reveal the significance of direct terrestrial inputs of organic
carbon and dissolved CO_2 in controlling riverine carbon cycle. Over the study period, the
Yangtze River watershed suffered severe soil erosion, averaging $2167 \text{ t km}^{-2} \text{ yr}^{-1}$ (Wang et al.,
2007b). Huge amounts of carbon were transported into the river system via erosion (Wu et al.,

400 2007). Decomposition of the terrestrial-origin organic carbon has resulted in the CO₂ excess in the headwater streams (Li et al., 2012).

Figure 8

The decreasing $p\text{CO}_2$ with increasing stream order imply continued CO₂ evasion along the river continuum and reduced supply of fresh CO₂. Except the three lakes connected to the mainstem
405 (Fig. 1a), the Yangtze River network is largely confined to its channel. Without large floodplains supplying labile organic matter to sustain high $p\text{CO}_2$ as in the Amazon River (Mayorga et al., 2005), its $p\text{CO}_2$ decreased progressively from the headwaters towards the mainstem channel. In addition, it is interesting to note that the $p\text{CO}_2$ in the highest three orders was equivalent (~1800 μatm ; Fig. 8). Instead of continuous decline, the stable $p\text{CO}_2$ suggests a balance between CO₂ evasion and supply of fresh CO₂ from upstream catchments or aquatic respiration. Contrary to
410 the headwater streams with close contact with terrestrial ecosystems, the downstream large streams and rivers are far away from rapid fresh CO₂ input. Moreover, these large streams and rivers are generally characterized by comparatively low gas transfer velocities due to weakened turbulence and mixing with benthic substrates (Butman and Raymond, 2011; Borges et al., 2015),
415 which can effectively inhibit CO₂ degassing and therefore maintain the balance. An example is the Yangtze estuary that presents considerably low CO₂ evasion fluxes of 16–34 mol m⁻² yr⁻¹, despite its significantly higher riverine $p\text{CO}_2$ than the overlying atmosphere (Zhai et al., 2007).

It is important to note, however, that the delineated 8 stream orders may not necessarily represent
420 the actual stream network. Limited by spatial resolution, the smallest headwater streams might

have been missed from the identified river network. In addition, these headwater streams are also generally absent of sampling stations. With much closer biogeochemical interactions with land ecosystems, these missed headwater streams tend to have higher $p\text{CO}_2$ (Benstead and Leigh, 2012; Aufdenkampe et al., 2011; Butman and Raymond, 2011). Thus, the actual $p\text{CO}_2$ gradient
425 along the stream order may be sharper if a higher $p\text{CO}_2$ in the headwater streams is included.

4.4 Implications for riverine CO_2 evasion

As mentioned earlier, riverine carbon transport has been a significant component of carbon cycle. Quantifying riverine carbon export is essential to better evaluate global carbon budget and
430 elucidate the magnitude of carbon exchange between different pools. For the estimation of CO_2 evasion, riverine $p\text{CO}_2$ denotes CO_2 concentration gradient across the water-air interface and thus the potential of CO_2 exchange. Prior studies indicate that elevated riverine $p\text{CO}_2$ can enhance CO_2 evasion owing to a steeper concentration gradient and a greater CO_2 availability for degassing (Long et al., 2015; Billett and Moore, 2008). When assessing global-scale CO_2 evasion,
435 however, the spatial distribution of $p\text{CO}_2$ is heavily skewed towards Northern America, Europe, and Australia (e.g., Lauerwald et al., 2015; Raymond et al., 2013), while data for Asian rivers are extremely lacking. This absence of an equally distributed $p\text{CO}_2$ database has made it challenging to accurately estimate global CO_2 evasion. The role of Asian rivers in global carbon export explicitly demonstrates that under-representation of Asian rivers would cause huge biases.

440

Comparing the Yangtze River with other rivers shows that its $p\text{CO}_2$ is higher than most world rivers (Table 4). The average $p\text{CO}_2$ of 2662 μatm suggests that the Yangtze River waters are potentially a prominent carbon source for the atmosphere. Large CO_2 evasion fluxes have been reported by several small-scale studies in the upper reach and the estuary (Zhai et al., 2007; Chen et al., 2008; Li et al., 2012), as also shown in Table 4. Nonetheless, a systematic estimation of CO_2 evasion from the whole Yangtze River network, including mainstem and its tributaries of all orders, remains lacking. This has hampered the assessment of its CO_2 evasion in a wider context linking the watershed's land-atmosphere and land-ocean carbon exchanges.

Table 4

Accelerated human activity is another urgent issue to be considered when investigating its riverine $p\text{CO}_2$ and CO_2 evasion. Approximately 50,000 dams, including the world's largest reservoir (i.e., the Three Gorges Reservoir; TGR), have been constructed in recent decades (Xu and Milliman, 2009). Assessing the impacts of dam-triggered changes to flow regime and biogeochemical processes on $p\text{CO}_2$ and CO_2 evasion is particularly important for deeper insights into its riverine carbon cycle (Table 4). For example, while the $p\text{CO}_2$ at Datong station declined continuously before the TGR impoundment (Fig. 4a; Wang et al., 2007a), our recent field survey shows that it has recovered from 1440 μatm in the 1980s to present 1700 μatm (see Fig. 4a). As for CO_2 degassing, recent work in the TGR indicates that its CO_2 evasion fluxes are different from natural rivers and are higher than other temperate reservoirs (Table 4; Zhao et al., 2013). Future research efforts are warranted to conduct systematic monitoring and evasion estimation.

Given the Yangtze River's role in global carbon export, a comprehensive assessment of CO₂ evasion is also meaningful for global carbon budget.

Conclusions

465 By using long-term water chemistry data measured in the Yangtze River watershed during the period 1960s–1985, we calculated its $p\text{CO}_2$ from pH and alkalinity. The pH in the Yangtze River waters varied from 6.5 to 9.2 and the alkalinity ranged from 415 to >3400 $\mu\text{eq L}^{-1}$ with high alkalinity concentrations occurring in carbonate-rich tributary catchments. Except one station in the upper reach showing a lower $p\text{CO}_2$ than the atmosphere, the Yangtze River waters were
470 supersaturated with dissolved CO₂, generally 2–20 folds the atmospheric equilibrium. Averaged over all stations, the basin-wide $p\text{CO}_2$ was 2662 ± 1240 μatm . As an important parameter for CO₂ evasion estimation, its $p\text{CO}_2$ was characterized by significant spatial and temporal variability, which was collectively controlled by carbon inputs from terrestrial ecosystems, hydrological regime, and rock weathering. High $p\text{CO}_2$ values were observed spatially in catchments with
475 abundant carbonate presence and seasonally in the wet season when recent-fixed organic matter was flushed into the river network. Decomposition of organic matter by microbial activity in aquatic systems facilitated CO₂ production and sustained the high $p\text{CO}_2$ values in wet seasons, although the alkalinity presented a significant dilution effect with water discharge. In addition, the $p\text{CO}_2$ decreased with increasing stream orders from the smallest headwater streams through
480 tributaries to the mainstem channel. A higher $p\text{CO}_2$ in the headwater streams illustrated the

influence of direct inputs of terrestrially-derived organic matter and weathering products via erosion and flushing on riverine carbon dynamics.

The substantially higher $p\text{CO}_2$ than the atmosphere indicated a potential of significant CO_2 emissions from the Yangtze River fluvial network. Quantifying the amount of CO_2 evasion should be a top priority, upon which its biogeochemical implications for watershed-scale carbon cycle can be assessed in association with carbon burial and downstream export. Given the extensive and intensive human disturbances within the watershed since the 1990s, special attention must be paid to the resulting changes to riverine $p\text{CO}_2$ and CO_2 evasion. A comparative analysis involving CO_2 evasion before large-scale human impacts and recent degassing estimates (e.g., Li et al., 2012; Liu et al., 2016) will be able to examine the anthropogenic perturbations of the river-atmosphere CO_2 fluxes due to damming and land-use change. Considering the Yangtze River's relevance to global carbon export, quantifying its CO_2 evasion is also of paramount importance for better assessments of global carbon budget.

Acknowledgements: This work was financially supported by the University of Hong Kong (grant no: 201612159004) and the National University of Singapore (grant no: R-109-000-172-646). We gratefully thank the two anonymous reviewers for their constructive comments that greatly improved the manuscript.

500

References

- Abril, G., Martinez, J.-M., Artigas, L. F., Moreira-Turcq, P., Benedetti, M. F., Vidal, L., Meziane, T., Kim, J.-H., Bernardes, M. C., and Savoye, N.: Amazon River carbon dioxide outgassing fuelled by wetlands, *Nature*, 505, 395-398, 2014.
- 505 Abril, G., Bouillon, S., Darchambeau, F., Teodoru, C., Marwick, T., Tamooh, F., Omengo, F., Geraert, N., Deirmendjian, L., Polensaere, P., and Borges, A. V.: Technical Note: Large

- overestimation of $p\text{CO}_2$ calculated from pH and alkalinity in acidic, organic-rich freshwaters, *Biogeosciences*, 12, 67-78, 2015.
- 510 Alekin, O. A., Semenov, A. D., and Skopintsev, B. A.: Handbook of Chemical Analysis of Land Waters, Gidrometeoizdat, St. Petersburg, Russia, 1973.
- Alin, S. R., Rasera, M. d. F. F. L., Salimon, C. I., Richey, J. E., Holtgrieve, G. W., Krusche, A. V., and Snidvongs, A.: Physical controls on carbon dioxide transfer velocity and flux in low-gradient river systems and implications for regional carbon budgets, *Journal of Geophysical Research*, 116, G01009, doi:10.1029/2010jg001398, 2011.
- 515 American Public Health Association (APHA): Standard Methods for the Examination of Water and Wastewater, 16th edition, American Public Health Association, Washington, DC, 1985.
- Amiotte-Suchet, P. A., Probst, J. L., and Ludwig, W.: Worldwide distribution of continental rock lithology: Implications for the atmospheric/soil CO_2 uptake by continental weathering and alkalinity river transport to the oceans, *Global Biogeochemical Cycles*, 17, 1038, doi:10.1029/2002gb001891, 2003.
- 520 Aufdenkampe, A. K., Mayorga, E., Raymond, P. A., Melack, J. M., Doney, S. C., Alin, S. R., Aalto, R. E., and Yoo, K.: Riverine coupling of biogeochemical cycles between land, oceans, and atmosphere, *Front Ecol Environ*, 9, 53-60, 2011.
- Bao, H., Wu, Y., and Zhang, J.: Spatial and temporal variation of dissolved organic matter in the Changjiang: fluvial transport and flux estimation, *Journal of Geophysical Research: Biogeosciences*, 120, 1870-1886, 2015.
- 525 Barros, N., Cole, J. J., Tranvik, L. J., Prairie, Y. T., Bastviken, D., Huszar, V. L., Del Giorgio, P., and Roland, F.: Carbon emission from hydroelectric reservoirs linked to reservoir age and latitude, *Nat Geosci*, 4, 593-596, 2011.
- 530 Battin, T. J., Luysaert, S., Kaplan, L. A., Aufdenkampe, A. K., Richter, A., and Tranvik, L. J.: The boundless carbon cycle, *Nat Geosci*, 2, 598-600, 2009.
- Benstead, J. P., and Leigh, D. S.: An expanded role for river networks, *Nature Geosci*, 5, 678-679, 2012.
- Billett, M., and Moore, T.: Supersaturation and evasion of CO_2 and CH_4 in surface waters at Mer Bleue peatland, Canada, *Hydrological Processes*, 22, 2044-2054, 2008.
- 535 Borges, A. V., Darchambeau, F., Teodoru, C. R., Marwick, T. R., Tamooh, F., Geeraert, N., Omengo, F. O., Guérin, F., Lambert, T., and Morana, C.: Globally significant greenhouse-gas emissions from African inland waters, *Nat Geosci*, 8, 637-642, 2015.
- Butman, D., and Raymond, P. A.: Significant efflux of carbon dioxide from streams and rivers in the United States, *Nat Geosci*, 4, 839-842, 2011.
- 540 Cauwet, G., and Mackenzie, F. T.: Carbon inputs and distribution in estuaries of turbid rivers: the Yang Tze and Yellow rivers (China), *Marine Chemistry*, 43, 235-246, 1993.
- Chen, C.-T. A., Zhai, W., and Dai, M.: Riverine input and air-sea CO_2 exchanges near the Changjiang (Yangtze River) Estuary: status quo and implication on possible future changes in metabolic status, *Continental Shelf Research*, 28, 1476-1482, 2008.
- 545 Chen, J., Wang, F. Y., Xia, X. H., and Zhang, L. T.: Major element chemistry of the Changjiang (Yangtze River), *Chemical Geology*, 187, 231-255, 2002.

- Chetelat, B., Liu, C. Q., Zhao, Z., Wang, Q., Li, S., Li, J., and Wang, B.: Geochemistry of the dissolved load of the Changjiang Basin rivers: anthropogenic impacts and chemical weathering, *Geochimica et Cosmochimica Acta*, 72, 4254-4277, 2008.
- 550 Cole, J. J., Prairie, Y. T., Caraco, N. F., McDowell, W. H., Tranvik, L. J., Striegl, R. G., Duarte, C. M., Kortelainen, P., Downing, J. A., Middelburg, J. J., and Melack, J.: Plumbing the global carbon cycle: Integrating inland waters into the terrestrial carbon budget, *Ecosystems*, 10, 171-184, 2007.
- 555 Duan, S., Xu, F., and Wang, L.-J.: Long-term changes in nutrient concentrations of the Changjiang River and principal tributaries, *Biogeochemistry*, 85, 215-234, 2007.
- Dubois, K. D., Lee, D., and Veizer, J.: Isotopic constraints on alkalinity, dissolved organic carbon, and atmospheric carbon dioxide fluxes in the Mississippi River, *Journal of Geophysical Research: Biogeosciences*, 115, 2010.
- 560 Gan, W. B., Chen, H. M., and Hart, Y. F.: Carbon transport by the Yangtze (at Nanjing) and Huanghe (at Jinan) Rivers, People's Republic of China, in: *Transport of Carbon and Minerals in Major World Rivers, Part 2*, edited by: E.T. Degens, S. Kempe, and Soliman, H., Mitt. Geol. Paläontol. Inst. Univ. Hamburg, SCOPE/UNEP Sonderbd., 459-470, 1983.
- Goudie, A. S., and Viles, H. A.: Weathering and the global carbon cycle: Geomorphological perspectives, *Earth-Science Reviews*, 113, 59-71, 2012.
- 565 Hope, D., Billett, M., and Cresser, M.: A review of the export of carbon in river water: fluxes and processes, *Environmental Pollution*, 84, 301-324, 1994.
- Humborg, C., Mörth, C., Sundbom, M., Borg, H., Blenckner, T., Giesler, R., and Ittekkot, V.: CO₂ supersaturation along the aquatic conduit in Swedish watersheds as constrained by
- 570 terrestrial respiration, aquatic respiration and weathering, *Global Change Biology*, 16, 1966-1978, 2010.
- Hunt, C., Salisbury, J., and Vandemark, D.: Contribution of non-carbonate anions to total alkalinity and overestimation of *p*CO₂ in New England and New Brunswick rivers, *Biogeosciences*, 8, 3069-3076, 2011.
- 575 Ittekkot, V.: Global trends in the nature of organic matter in river suspensions, *Nature*, 332, 436-438, 1988.
- Kemenes, A., Forsberg, B. R., and Melack, J. M.: CO₂ emissions from a tropical hydroelectric reservoir (Balbina, Brazil), *Journal of Geophysical Research*, 116, G03004, doi:10.1029/2010JG001465, 2011.
- 580 Laruelle, G. G., Dürr, H., Lauerwald, R., Hartmann, J., Slomp, C., Goossens, N., and Regnier, P.: Global multi-scale segmentation of continental and coastal waters from the watersheds to the continental margins, *Hydrol Earth Syst Sc*, 17, 2029-2051, 2013.
- Lauerwald, R., Hartmann, J., Moosdorf, N., Kempe, S., and Raymond, P. A.: What controls the spatial patterns of the riverine carbonate system? –A case study for North America, *Chemical*
- 585 *Geology*, 337-338, 114-127, 2013.
- Lauerwald, R., Laruelle, G. G., Hartmann, J., Ciais, P., and Regnier, P. A.: Spatial patterns in CO₂ evasion from the global river network, *Global Biogeochemical Cycles*, 29, 534-554, 2015.

- Lewis, E., and Wallace, D. W. R.: Program developed for CO₂ system calculations. ORNL/CDIAC-105, Carbon dioxide Information Analysis Center, Oak Ridge National Laboratory, Oak Ridge, TN., 1998.
- 590 Li, S.-L., Liu, C.-Q., Li, J., Lang, Y.-C., Ding, H., and Li, L.: Geochemistry of dissolved inorganic carbon and carbonate weathering in a small typical karstic catchment of Southwest China: Isotopic and chemical constraints, *Chemical Geology*, 277, 301-309, 2010a.
- Li, S., Cheng, X., Xu, Z., Han, H., and Zhang, Q.: Spatial and temporal patterns of the water quality in the Danjiangkou Reservoir, China, *Hydrological sciences journal*, 54, 124-134, 2009.
- 595 Li, S., Lu, X. X., He, M., Zhou, Y., Li, L., and Ziegler, A. D.: Daily CO₂ partial pressure and CO₂ outgassing in the upper Yangtze River basin: A case study of the Longchuan River, China, *Journal of Hydrology*, 466-467, 141-150, 2012.
- Li, S., Lu, X., and Bush, R. T.: CO₂ partial pressure and CO₂ emission in the Lower Mekong River, *Journal of Hydrology*, 504, 40-56, 2013.
- 600 Li, X.-D., Liu, C.-Q., Harue, M., Li, S.-L., and Liu, X.-L.: The use of environmental isotopic (C, Sr, S) and hydrochemical tracers to characterize anthropogenic effects on karst groundwater quality: A case study of the Shuicheng Basin, SW China, *Appl Geochem*, 25, 1924-1936, 2010b.
- 605 Liu, S., Lu, X. X., Xia, X., Zhang, S., Ran, L., Yang, X., and Liu, T.: Dynamic biogeochemical controls on river pCO₂ and recent changes under aggravating river impoundment: an example of the subtropical Yangtze River, *Global Biogeochemical Cycles*, 30, 880-897, 2016.
- Long, H., Vihermaa, L., Waldron, S., Hoey, T., Quemin, S., and Newton, J.: Hydraulics are a first-order control on CO₂ efflux from fluvial systems, *Journal of Geophysical Research: Biogeosciences*, 120, 1912-1922, 2015.
- 610 Lynch, J. K., Beatty, C. M., Seidel, M. P., Jungst, L. J., and DeGrandpre, M. D.: Controls of riverine CO₂ over an annual cycle determined using direct, high temporal resolution pCO₂ measurements, *Journal of Geophysical Research*, 115, G03016, doi:10.1029/2009jg001132, 2010.
- 615 Marcé, R., Obrador, B., Morguá, J.-A., Riera, J. L., López, P., and Armengol, J.: Carbonate weathering as a driver of CO₂ supersaturation in lakes, *Nat Geosci*, 8, 107-111, 2015.
- Mayorga, E., Aufdenkampe, A. K., Masiello, C. A., Krusche, A. V., Hedges, J. I., Quay, P. D., Richey, J. E., and Brown, T. A.: Young organic matter as a source of carbon dioxide outgassing from Amazonian rivers, *Nature*, 436, 538-541, 2005.
- 620 Milliman, J. D., Qinchun, X., and Zuosheng, Y.: Transfer of particulate organic carbon and nitrogen from the Yangtze River to the ocean, *American Journal of Science*, 284, 824-834, 1984.
- Ran, L., Lu, X. X., Richey, J. E., Sun, H., Han, J., Liao, S., and Yi, Q.: Long-term spatial and temporal variation of CO₂ partial pressure in the Yellow River, China, *Biogeosciences*, 12, 921-932, 2015a.
- 625 Ran, L., Lu, X. X., Yang, H., Li, L., Yu, R., Sun, H., and Han, J.: CO₂ outgassing from the Yellow River network and its implications for riverine carbon cycle, *Journal of Geophysical Research: Biogeosciences*, 120, 1334-1347, 2015b.

- 630 Raymond, P. A., Caraco, N. F., and Cole, J. J.: Carbon dioxide concentration and atmospheric
flux in the Hudson River, *Estuaries*, 20, 381-390, 1997.
- Raymond, P. A., Bauer, J. E., and Cole, J. J.: Atmospheric CO₂ evasion, dissolved inorganic
carbon production, and net heterotrophy in the York River estuary, *Limnology and
Oceanography*, 45, 1707-1717, 2000.
- 635 Raymond, P. A., and Cole, J. J.: Increase in the export of alkalinity from North America's largest
river, *Science*, 301, 88-91, 2003.
- Raymond, P. A., Hartmann, J., Lauerwald, R., Sobek, S., McDonald, C., Hoover, M., Butman,
D., Striegl, R., Mayorga, E., and Humborg, C.: Global carbon dioxide emissions from inland
waters, *Nature*, 503, 355-359, 2013.
- 640 Regnier, P., Friedlingstein, P., Ciais, P., Mackenzie, F. T., Gruber, N., Janssens, I. A., Laruelle,
G. G., Lauerwald, R., Luysaert, S., and Andersson, A. J.: Anthropogenic perturbation of the
carbon fluxes from land to ocean, *Nat Geosci*, 6, 597-607, 2013.
- Richey, J. E., Melack, J. M., Aufdenkampe, A. K., Ballester, V. M., and Hess, L. L.: Outgassing
from Amazonian rivers and wetlands as a large tropical source of atmospheric CO₂, *Nature*,
416, 617-620, 2002.
- 645 Sarma, V. V. S. S., Kumar, N. A., Prasad, V. R., Venkataramana, V., Appalanaidu, S., Sridevi,
B., Kumar, B. S. K., Bharati, M. D., Subbaiah, C. V., Acharyya, T., Rao, G. D., Viswanadham,
R., Gawade, L., Manjary, D. T., Kumar, P. P., Rajeev, K., Reddy, N. P. C., Sarma, V. V.,
Kumar, M. D., Sadhuram, Y., and Murty, T. V. R.: High CO₂ emissions from the tropical
Godavari estuary (India) associated with monsoon river discharges, *Geophys Res Lett*, 38,
650 L08601, doi:10.1029/2011gl046928, 2011.
- Schlünz, B., and Schneider, R. R.: Transport of terrestrial organic carbon to the oceans by rivers:
re-estimating flux- and burial rates, *Int J Earth Sci*, 88, 599-606, 2000.
- Syvitski, J. P. M., Vorosmarty, C. J., Kettner, A. J., and Green, P.: Impact of humans on the flux
of terrestrial sediment to the global coastal ocean, *Science*, 308, 376-380, 2005.
- 655 Telmer, K., and Veizer, J.: Carbon fluxes, pCO₂ and substrate weathering in a large northern
river basin, Canada: carbon isotope perspectives, *Chemical Geology*, 159, 61-86, 1999.
- Teodoru, C., Nyoni, F., Borges, A., Darchambeau, F., Nyambe, I., and Bouillon, S.: Dynamics of
greenhouse gases (CO₂, CH₄, N₂O) along the Zambezi River and major tributaries, and their
importance in the riverine carbon budget, *Biogeosciences*, 12, 2431-2453, 2015.
- 660 Wallin, M. B., Grabs, T., Buffam, I., Laudon, H., Ågren, A., Öquist, M. G., and Bishop, K.:
Evasion of CO₂ from streams—The dominant component of the carbon export through the
aquatic conduit in a boreal landscape, *Global Change Biology*, 19, 785-797, 2013.
- Wallin, M. B., Löfgren, S., Erlandsson, M., and Bishop, K.: Representative regional sampling of
carbon dioxide and methane concentrations in hemiboreal headwater streams reveal
665 underestimates in less systematic approaches, *Global Biogeochemical Cycles*, 28, 465-479,
2014.
- Wang, F. S., Wang, Y. C., Zhang, J., Xu, H., and Wei, X. G.: Human impact on the historical
change of CO₂ degassing flux in River Changjiang, *Geochem T*, 8, doi:10.1186/1467-4866-8-7,
2007a.

- 670 Wang, F. S., Wang, B. L., Liu, C. Q., Wang, Y. C., Guan, J., Liu, X. L., and Yu, Y. X.: Carbon dioxide emission from surface water in cascade reservoirs-river system on the Maotiao River, southwest of China, *Atmos Environ*, 45, 3827-3834, 2011.
- Wang, X., Ma, H., Li, R., Song, Z., and Wu, J.: Seasonal fluxes and source variation of organic carbon transported by two major Chinese Rivers: The Yellow River and Changjiang (Yangtze) River, *Global Biogeochemical Cycles*, 26, GB2025, doi:10.1029/2011gb004130, 2012.
- 675 Wang, Z. Y., Li, Y., and He, Y.: Sediment budget of the Yangtze River, *Water Resour Res*, 43, W04401, doi:10.1029/2006WR005012, 2007b.
- Wanninkhof, R., Park, G.-H., Takahashi, T., Sweeney, C., Feely, R. A., Nojiri, Y., Gruber, N., Doney, S. C., McKinley, G. A., and Lenton, A.: Global ocean carbon uptake: magnitude, variability and trends, *Biogeosciences*, 10, 1983-2000, 2013.
- 680 Weyhenmeyer, G. A., Kosten, S., Wallin, M. B., Tranvik, L. J., Jeppesen, E., and Roland, F.: Significant fraction of CO₂ emissions from boreal lakes derived from hydrologic inorganic carbon inputs, *Nat Geosci*, 8, 933-936, 2015.
- Wu, Y., Zhang, J., Liu, S. M., Zhang, Z. F., Yao, Q. Z., Hong, G. H., and Cooper, L.: Sources and distribution of carbon within the Yangtze River system, *Estuar Coast Shelf S*, 71, 13-25, 2007.
- 685 Xu, K., and Milliman, J. D.: Seasonal variations of sediment discharge from the Yangtze River before and after impoundment of the Three Gorges Dam, *Geomorphology*, 104, 276-283, 2009.
- Yang, S., Zhao, Q., and Belkin, I. M.: Temporal variation in the sediment load of the Yangtze river and the influences of human activities, *Journal of Hydrology*, 263, 56-71, 2002.
- 690 Yao, G. R., Gao, Q. Z., Wang, Z. G., Huang, X. K., He, T., Zhang, Y. L., Jiao, S. L., and Ding, J.: Dynamics of CO₂ partial pressure and CO₂ outgassing in the lower reaches of the Xijiang River, a subtropical monsoon river in China, *Sci Total Environ*, 376, 255-266, 2007.
- Zhai, W. D., Dai, M. H., and Guo, X. G.: Carbonate system and CO₂ degassing fluxes in the inner estuary of Changjiang (Yangtze) River, China, *Marine Chemistry*, 107, 342-356, 2007.
- 695 Zhang, L., Xue, M., Wang, M., Cai, W.-J., Wang, L., and Yu, Z.: The spatiotemporal distribution of dissolved inorganic and organic carbon in the main stem of the Changjiang (Yangtze) River and the effect of the Three Gorges Reservoir, *Journal of Geophysical Research: Biogeosciences*, 119, 741-757, 2014.
- 700 Zhao, Y., Wu, B., and Zeng, Y.: Spatial and temporal patterns of greenhouse gas emissions from Three Gorges Reservoir of China, *Biogeosciences*, 10, 1219-1230, 2013.
- Zhu, T. X.: Gully and tunnel erosion in the hilly Loess Plateau region, China, *Geomorphology*, 153-154, 144-155, 2012.

705 Table 1. Comparison of alkalinity ($\mu\text{eq L}^{-1}$) and pH at Wuhan station between the GEMS/Water Programme results and the hydrological yearbooks, expressed as mean \pm standard error.

Item	1980	1981	1982	1983	1984	1984
GEMS/Water Programme						
Alkalinity	2050 \pm 286	2004 \pm 188	2000 \pm 232	1838 \pm 252	2200 \pm 247	1992 \pm 219
pH	7.83 \pm 0.16	7.73 \pm 0.24	8.04 \pm 0.09	8.06 \pm 0.05	8.00 \pm 0.09	7.88 \pm 0.06
Hydrological yearbooks						
Alkalinity	2310 \pm 314	2187 \pm 236	2274 \pm 268	2033 \pm 304	2383 \pm 277	2306 \pm 238
pH	7.93 \pm 0.09	7.87 \pm 09	8.01 \pm 0.09	7.94 \pm 0.08	7.93 \pm 0.10	7.98 \pm 0.08

Table 2. Riverine pH, alkalinity, and $p\text{CO}_2$ in the Yangtze River basin (median±standard deviation)^a.

River/tributary	Station	pH	Alkalinity	$p\text{CO}_2$
			$\mu\text{eq L}^{-1}$	μatm
Mainstem	Benzilan	8.29±0.11	2352±435	681±156
	Shigu	8.18±0.48	2544±438	846±262
	Jingjiangjie	8.11±0.12	2905±362	916±202
	Dukou	8.22±0.12	2399±429	826±197
	Longjie	8.23±0.17	2185±396	786±226
	Huatan	8.17±0.15	2237±418	882±287
	Pingshan	8.13±0.10	2215±407	1001±235
	Zhutuo	7.88±0.19	2299±349	2405±781
	Cuntan	8.08±0.11	2173±311	1087±319
	Yichang	7.95±0.15	2343±300	1653±469
	Luoshan	7.76±0.11	2280±248	2380±691
	Wuhan	7.93±0.11	2060±263	1521±497
	Datong	7.84±0.14	1919±312	1711±806
	Nanjing ^b	7.56±0.16	2339±339	3796±1623
Nanjing ^c	7.54±0.18	2296±357	3793±2186	
Major tributaries ^d				
Yalongjiang	Xiaodeshi	8.02±0.22	2576±465	1567±715
Daduhe	Fuluzhen	7.66±0.23	1909±289	2577±1620
Minjiang	Gaochang	8.02±0.15	1816±327	1020±525
Tuojiang	Lijiawan	8.01±0.11	2705±507	1504±572
Jialingjiang	Beibei	8.11±0.14	2289±509	1196±244
Wujiang	Wulong	8.01±0.14	2420±279	1361±508
Yuanjiang	Taoyuan	7.61±0.25	1822±480	2801±2144
Xiangjiang	Xiangtan	7.76±0.44	1739±331	2349±2521
Hanjiang	Xiaoshicun	7.93±0.13	2262±480	1715±536
Ganjiang	Waizhou	7.44±0.44	880±236	2205±2048
Yangtze basin ^e	1% percentile	7.03	556	788
	10% percentile	7.35	842	1236
	50% percentile	7.71	2237	2455
	90% percentile	8.05	3305	4344
	99% percentile	8.28	4437	6163

^aStation-based $p\text{CO}_2$ was summarized in Table S1; ^bAffected by high tides; ^cAffected by low tides; ^dMedian values of the data for the lowermost station on the mainstem of the specific tributary; ^eStatistics based on the measurements at the used 339 stations.

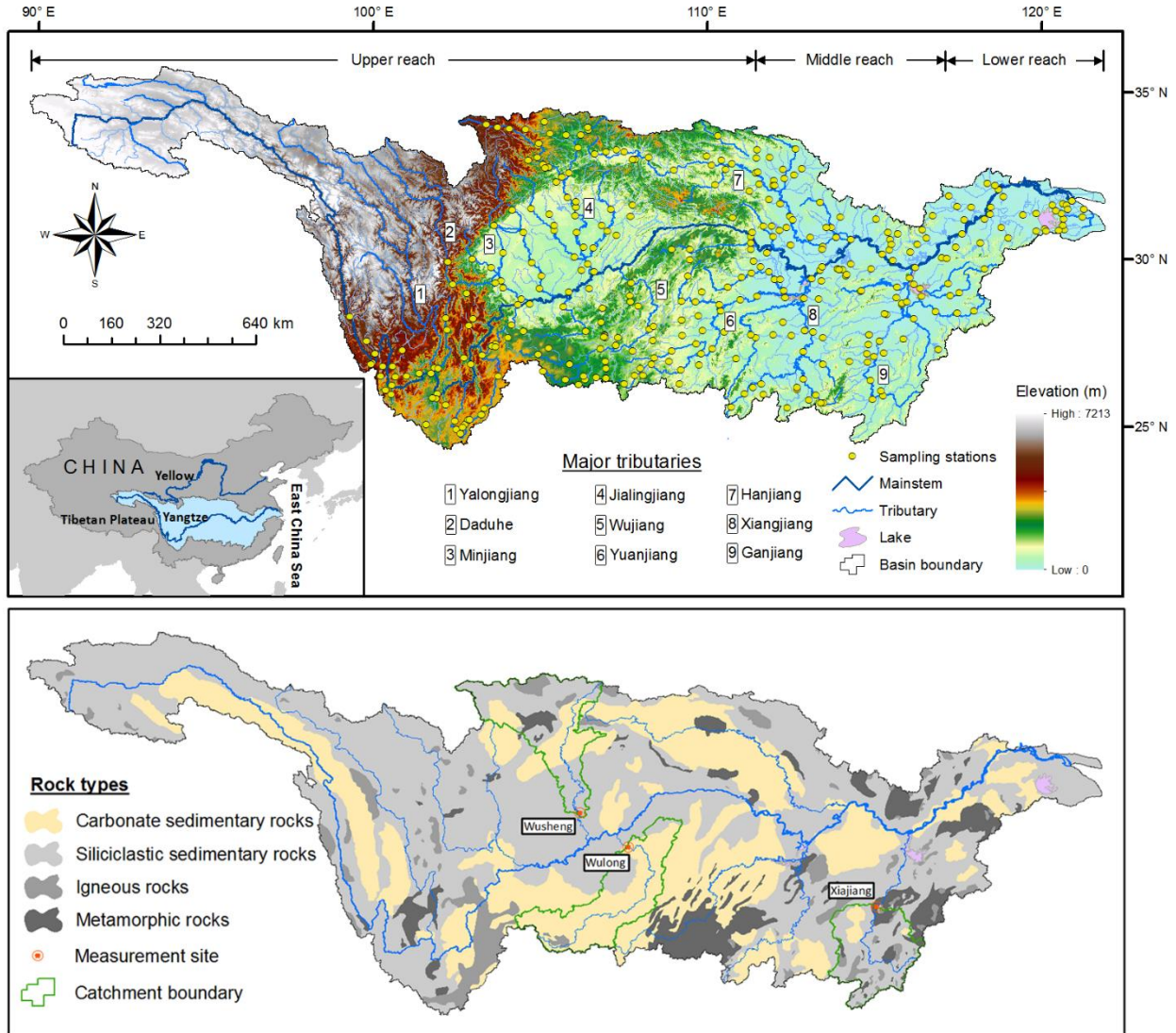
Table 3. Hydro-geochemical features of the Wujiang (Wulong station), Jialingjiang (Wusheng station), and Ganjiang (Xiajiang station) catchments.

Control station	Control area	Water discharge	pH	Alkalinity	$p\text{CO}_2$	Ca^{2+}	SiO_2	Sedimentary rock types (% of area)		
	km^2	$\text{m}^3 \text{s}^{-1}$		$\mu\text{eq L}^{-1}$	μatm	$\mu\text{mol L}^{-1}$	$\mu\text{mol L}^{-1}$	Carbonate	Siliciclastic	Igneous + metamorphic
Wulong	80,536	1570	7.72±0.14	3021±527	3537±1247	1145±278	59±31	82.9	14.8	2.3
Wusheng	80,550	793	7.80±0.21	2484±948	2671±490	1005±170	94±30	30.4	55.3	14.3
Xiajiang	62,387	1644	7.34±0.08	953±266	2642±626	242±91	105±18	9.1	64.7	26.2

715

Table 4. Comparison of $p\text{CO}_2$ and CO_2 evasion among world large rivers and typical reservoirs in the Yangtze River basin.

River	Country	Climate	$p\text{CO}_2$	CO_2 evasion	Reference
			μatm	$\text{mol m}^{-2} \text{yr}^{-1}$	
Yangtze network	China	Subtropical monsoon	2662±1240	/	This study
Upper Yangtze	China	Subtropical monsoon	2100	57	Li et al., 2012
Lower Yangtze	China	Subtropical monsoon	1297±901	14.2–54.4	Wang et al., 2007a
Yangtze estuary	China	Subtropical monsoon	650–1440	15.5–34.2	Zhai et al., 2007
Amazon	Brazil	Tropical	3929	162.2	Lauerwald et al. 2015
Ottawa	Canada	Temperate	1200	14.2	Telmer and Veizer, 1999
Hudson	USA	Temperate	1125±403	5.8–13.5	Raymond et al., 1997
York estuary	USA	Temperate	1070±867	6.3	Raymond et al., 2000
Mississippi	USA	Temperate	1335±130	98.5±32.5	Dubois et al., 2010
Yukon	Canada	Subarctic	582–705	11.6–21.2	Lauerwald et al., 2015
Yellow	China	Arid and semiarid	2810±1985	312.4±149.2	Ran et al., 2015b
Xijiang (Pearl)	China	Subtropical monsoon	2600	69.2–130	Yao et al., 2007
Mekong (>100 m wide rivers)	SE Asia	Tropical monsoon	703–1597	32–138	Alin et al., 2011
Godavari estuary	India	Tropical monsoon	<500–33,000	52.6	Sarma et al., 2011
Global rivers			2400	131.2	Lauerwald et al. 2015
<i>Typical reservoirs in the Yangtze River basin</i>					
Wujiang cascade reservoirs			38–3300	-3.3–32.5	Wang et al., 2011
Three Gorges Reservoir (TGR)			/	35.1	Zhao et al., 2013



720 Fig. 1. Maps of the Yangtze River basin showing sampling stations (top) and rock compositions (bottom). Rock information is modified from Chen et al. (2002) and Chetelat et al. (2008).

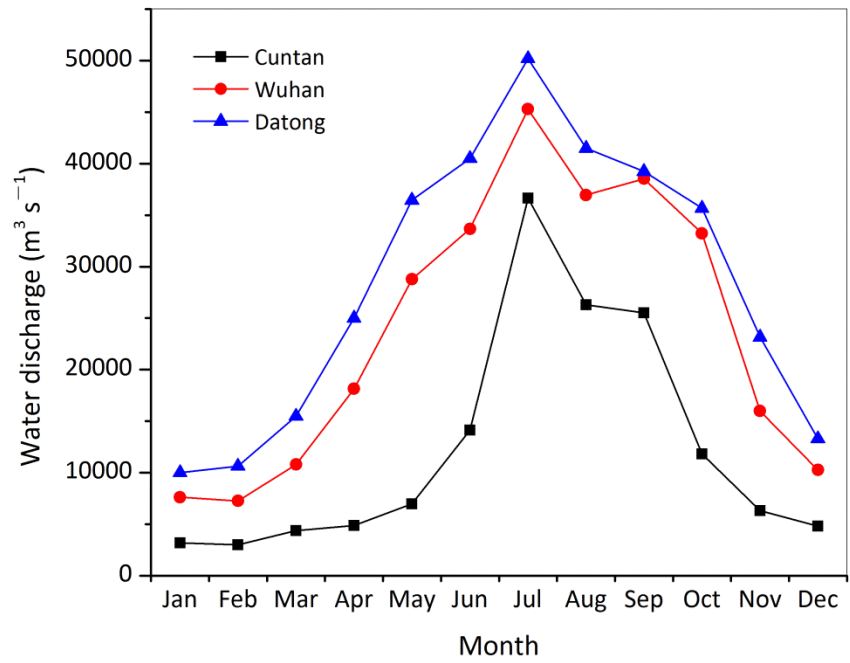


Fig. 2. Monthly variations in water discharge of the Yangtze River at Cuntan (upper reach), Wuhan (middle reach), and Datong stations (lower reach).

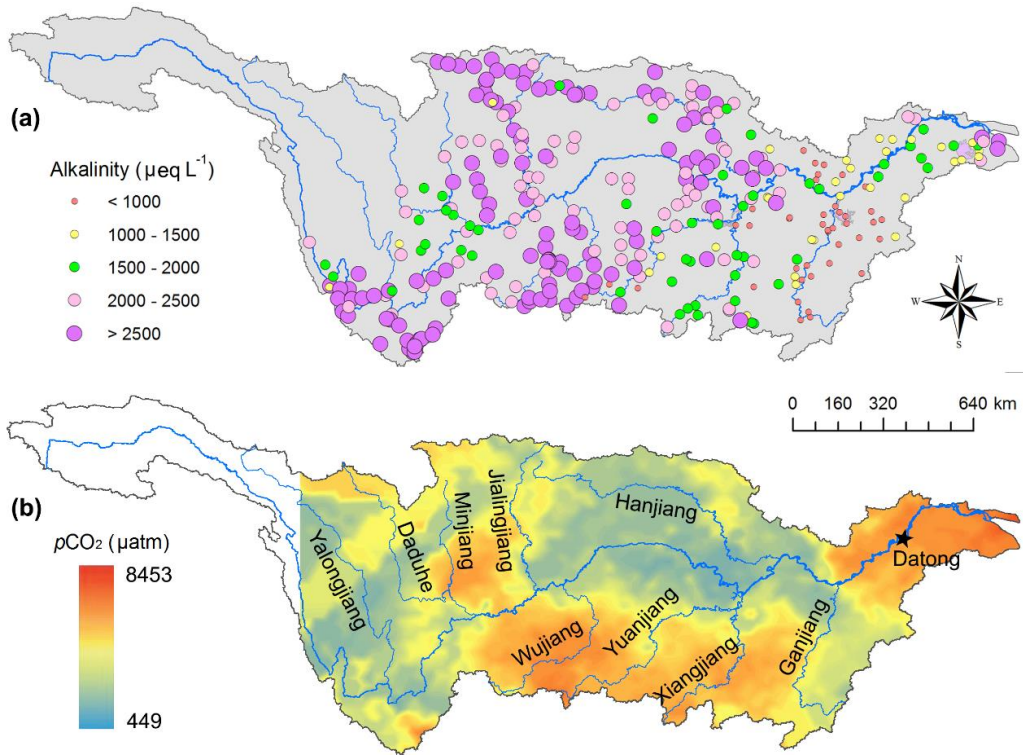


Fig. 3. Spatial distribution of alkalinity (a) and $p\text{CO}_2$ (b) in the Yangtze River basin. The headwater region in (b) was not interpolated because of insufficient stations.

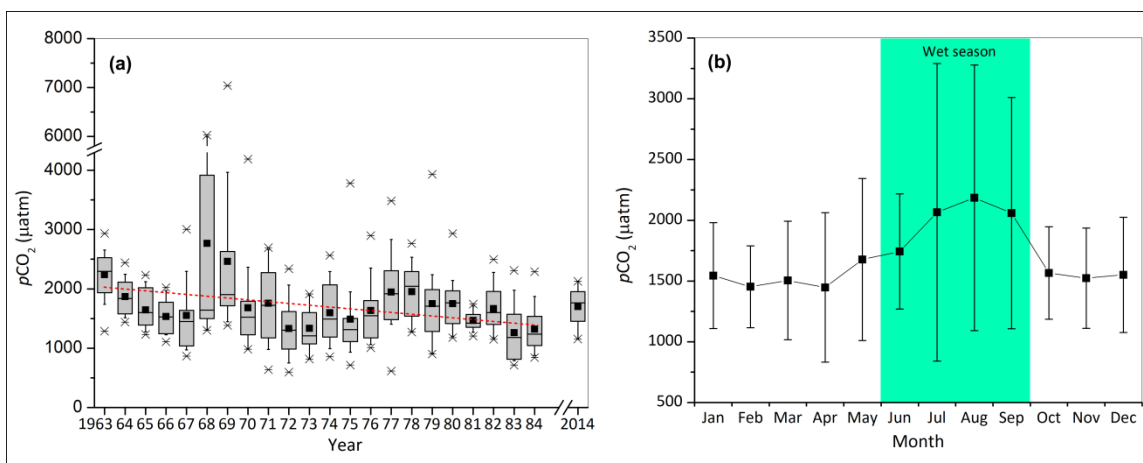
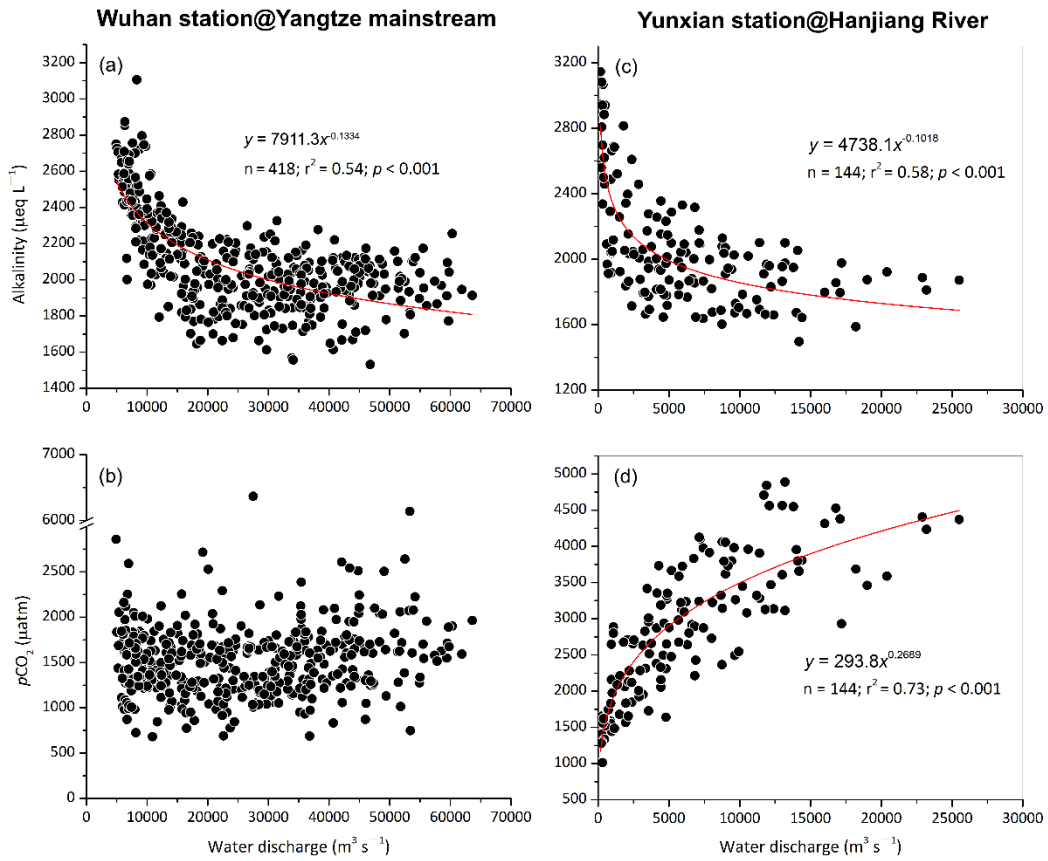
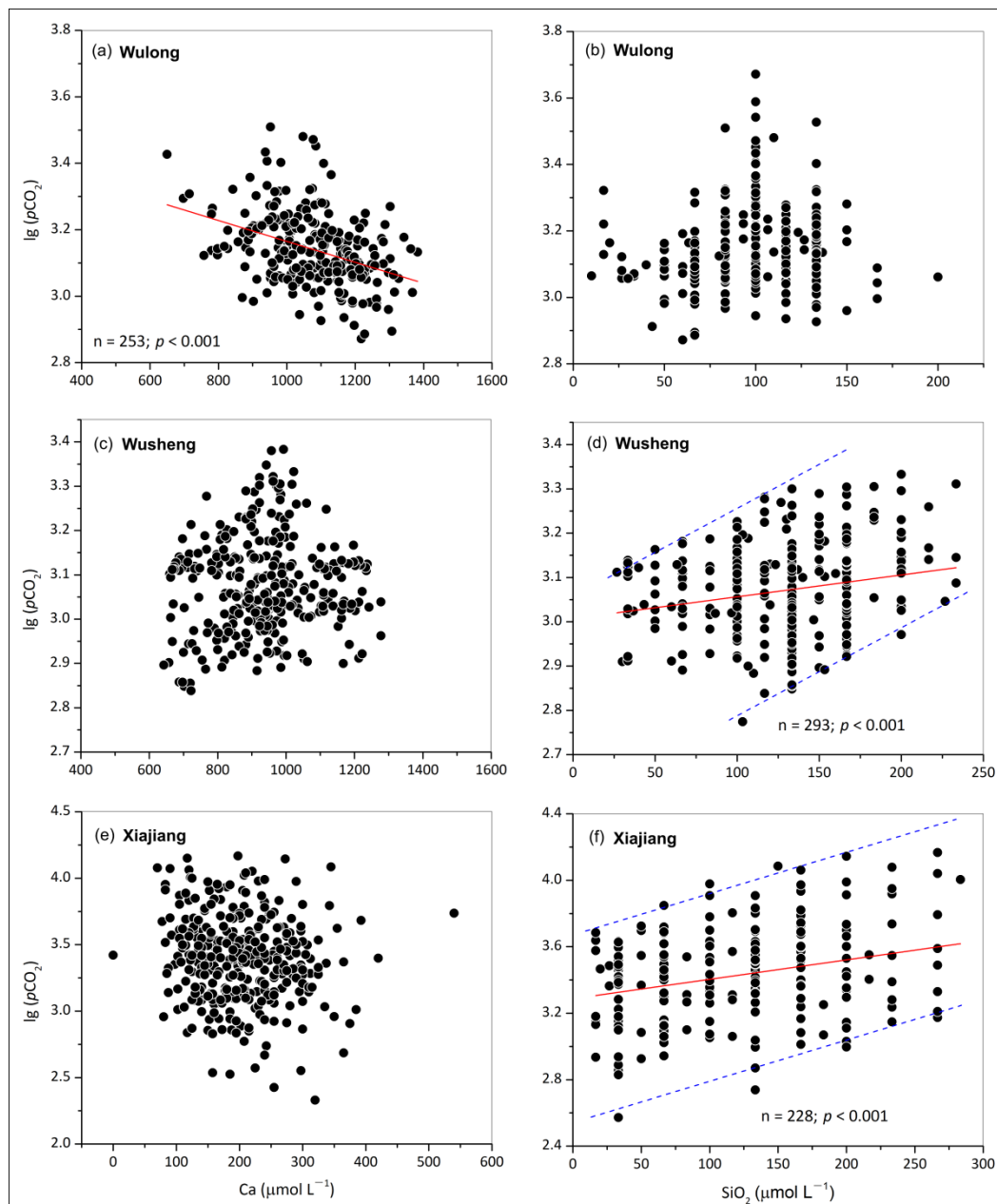


Fig. 4. Temporal variations of $p\text{CO}_2$ at Datong station. (a) box-and-whisker plot shows significant inter-annual changes; (b) seasonal variations. The dash line in (a) represents linear regression and the values for 2014 are derived from Liu et al. (2016). Error bars denote standard deviation.

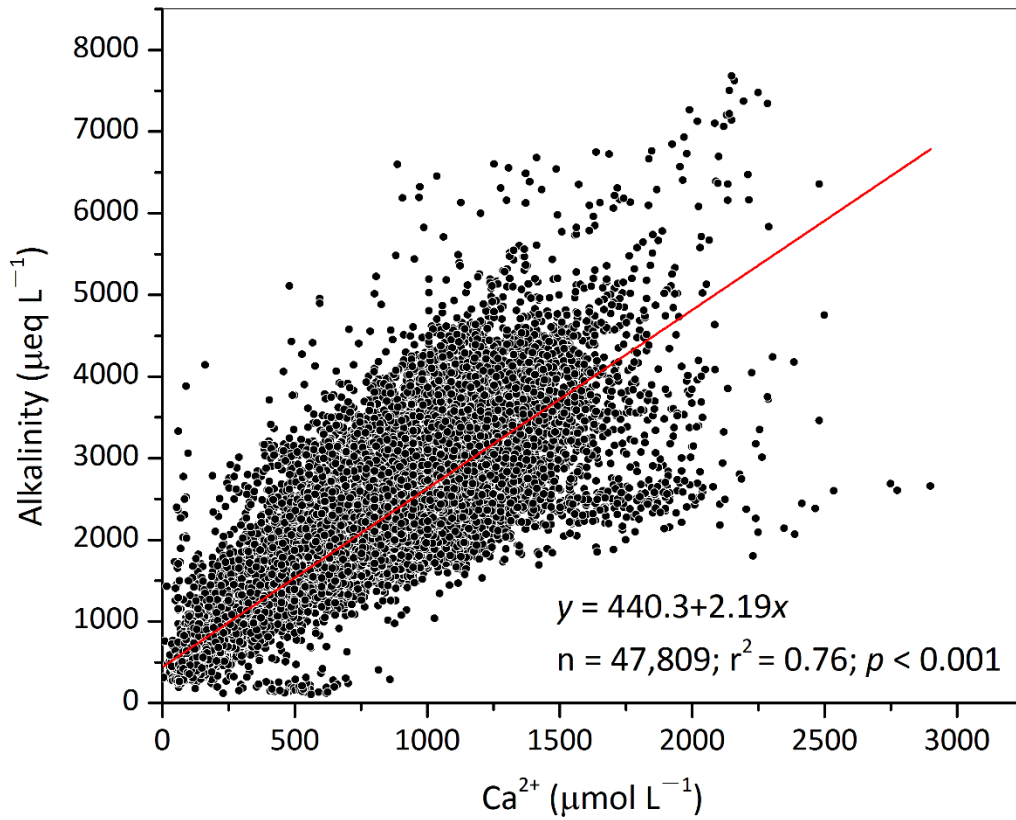
730



735 Fig. 5. Correlations between water discharge and instantaneous alkalinity and $p\text{CO}_2$: the mainstem at Wuhan station (a and b) and the Hanjiang River at Yunxian station (c and d).



740 Fig. 6. Responses of $p\text{CO}_2$ to rock weathering products in three typical catchments with distinct rock compositions: a–b: Wujiang River (Wulong station); b–c: Jialiangjiang River (Wusheng station); e–f: Ganjiang River (Xiajiang station). The solid lines represent linear regression.



745 Fig. 7. Strong correlation between chemical weathering, using Ca^{2+} as a proxy, and alkalinity.

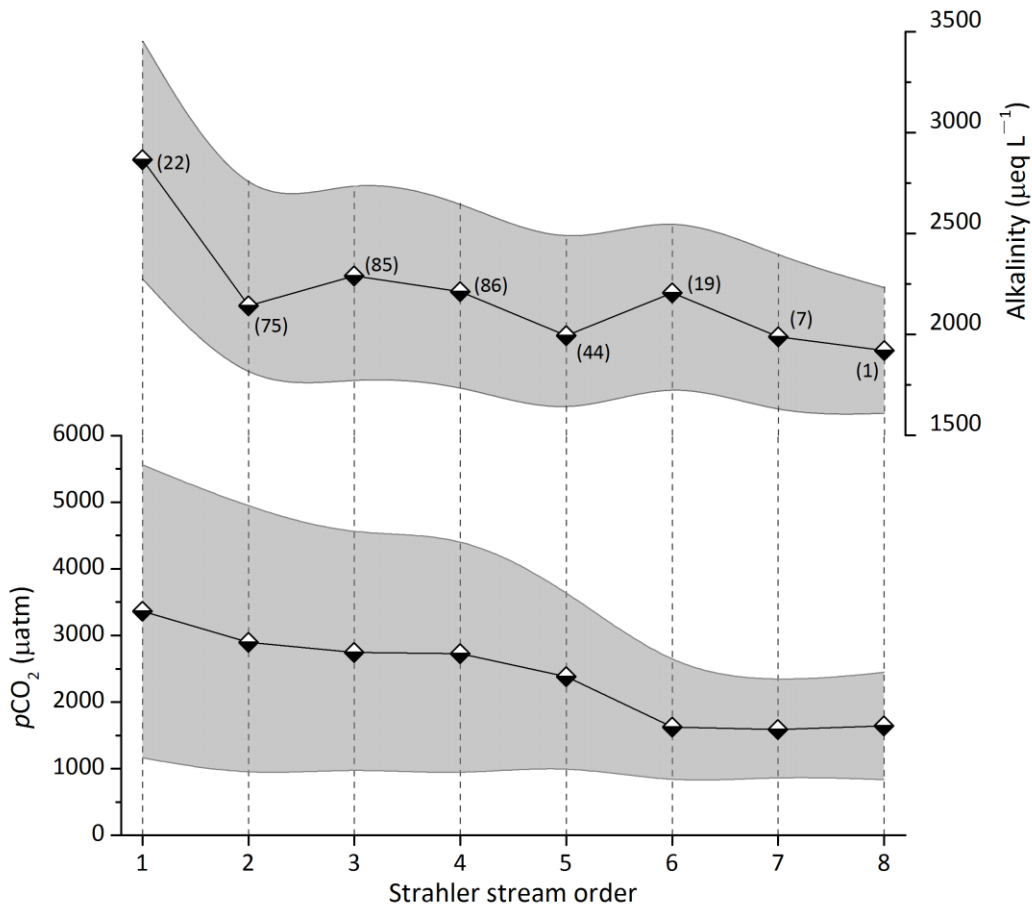


Fig. 8. Decreasing alkalinity (top) and $p\text{CO}_2$ (bottom) with increasing Strahler stream order. The grey shade denotes standard deviation and the numbers in parentheses represent the number of stations aggregated for each stream order.

750